Front. Environ. Sci. Eng. 2015, 9(5): 840–849
DOI 10.1007/s11783-015-0781-2

RESEARCH ARTICLE

Effect of Fe loading quantity on reduction reactivity of nano zero-valent iron supported on chelating resin

Jialu SHI, Shengnan YI, Chao LONG (✉), Aimin LI

State Key Laboratory of Pollution Control and Resource Reuse, School of the Environment, Nanjing University, Nanjing 210023, China

Abstract In this study, nanoscale zero-valent iron (NZVI) were immobilized within a chelating resin (DOW 3N). To investigate the effect of Fe loading on NZVI reactivity, three NZVI-resin composites with different Fe loading were obtained by preparing Fe(III) solution in 0, 30 and 70% (v/v) ethanol aqueous, respectively; the bromate was used as a model contaminant. TEM reveals that increasing the Fe loading resulted in much larger size and poor dispersion of nanoscale iron particles. The results indicated that the removal efficiency of bromate and the rate constant (K_{obs}) were decreased with increasing the Fe loading. For the NZVI-resin composite with lower Fe loading, the removal efficiency of bromate declined more significantly with the increase of DO concentrations. Under acidic conditions, decreasing the pH value had the most significant influence on NZVI-R3 with highest Fe loading for bromate removal; however, under alkaline conditions, the most significant influence of pH was on NZVI-R1 with lowest Fe loading. The effects of co-existing anions NO_3^-, PO_4^{3-} and HCO_3^- were also investigated. All of the co-existing anions showed the inhibition to bromate reduction.

Keywords nanoscale zero valent iron, loading quantity, reduction, chelating resin, bromated

1 Introduction

Due to the inexpensiveness, good availability and stability of nano zero valent iron (NZVI), it has been extensively studied as a strong reductant for removal of a wide variety of organics, such as trichloroethene [1,2], azo dye Acid Blue 113 [3], polychlorinated biphenyls [4], dinitrotoluene sulfonates [5], heavy metals including Pb^{2+} [6], Ni^{2+} [7], Cu^{2+} [8,9], and anions such as ClO_4^- [10,11], NO_3^- [12,13], and BrO_3^- [14–17]. These studies had demonstrated that NZVI exhibited good reduction reactivity for reducible contaminants, and hence was suggested to be one of the most competitive technologies for aqueous contaminants control.

Reduction of contaminants by NZVI particles is a surface-mediated process [15], therefore, it is believed that the particle size of iron would be one of the important parameters to the reaction rate [18]. Since the nano iron particles tend to agglomerate rapidly, some studies have tried to manipulate the size of prepared NZVI to enhance the reduction reactivity [1,19,20]. Using support materials to immobilize NZVI is one possible way to solve the above-mentioned problem. As reported in the literatures, active carbon [21,22], clay minerals [23], zeolite [24] and polymeric resin [25,26] have been successfully employed as supporters to control the size and morphology of iron nanoparticles. It is well-known that the removal capacity of supported NZVI is directly related to the Fe^0 loading. Moreover, high Fe loading is very favorable to reduce supporter usage and cut down production cost of NZVI composite. Therefore, it is generally expected to attain high Fe^0 loading quantity when the supported NZVI is prepared. However, to our knowledge, there is limited knowledge to evaluate the influence of Fe loading quantity on the nanoparticles size and reactive activity.

In this study, the chelating resin DOWEXTM M4195 (DOW 3N), composed of a polystyrene cross-linked with divinyl benzene and bis(2-pyridylmethyl)amine functional groups, was chosen as the supporter of NZVI particles. The previous study has proven that it was an excellent carrier for allowing anion and cation contaminants to diffuse freely into internal surface of polymer without Donnan co-ion exclusion effect [27]. The bromate, which is classified as high carcinogenic potential carcinogens by the International Agency for Research on Cancer (IARC) [28], was used as a model contaminant. To investigate the effect of Fe loading quantity on nanoparticles reactive activity, the nanoscale zero-valent iron supported on DOW 3N with different Fe loading quantity were prepared through Fe(III) solution in 0:100, 30:70 and 70:30 (v/v) ethanol-water

Received December 2, 2014; accepted February 25, 2015

E-mail: clong@nju.edu.cn

mixed solvent, respectively. The characterization of NZVI was obtained by high-resolution transmission electron microscope and XPS analysis. Removal efficiency of bromate was compared by three NZVI composites.

2 Material and methods

2.1 Chemicals

The DOWEX™ M4195 (DOW 3N) was purchased from Sigma Aldrich (Shanghai, China). Before use, the resins were extracted with ethanol in a Soxlet apparatus for 8 h, and then the resins were washed by 4 wt.% hydrochloric acid solution and 4 wt.% sodium hydroxide solutions in turn. The structure information of DOW 3N is listed in Table S1 of Supplementary material. All chemicals including ferric sulfate ($Fe_2(SO_4)_3$), sodium borohydride ($NaBH_4$), sodium nitrate ($NaNO_3$), sodium phosphate (Na_3PO_4), sodium bicarbonate ($NaHCO_3$) and sodium bromate ($NaBrO_3$) are analytical grade and used directly without further purification. All solutions were prepared using ultrapure water produced by a Millipore-Q system (Millipore Synergy, USA).

2.2 Preparation of resin-supported NZVI

The 3 $g \cdot L^{-1}$ of Fe^{3+} solution was prepared by dissolving ferric sulfate in 0:100, 30:70 and 70:30 (v/v) ethanol-water mixed solvent, respectively. The preparation of resin-supported NZVI included two steps: 1) Fe^{3+} was chelated on the DOW 3N; 2) the chelated Fe^{3+} was reduced to Fe^0 by $NaBH_4$. In detail, 0.5 g DOW 3N resin was first added into 250 mL ethanol-water solution containing 3 $g \cdot L^{-1}$ of Fe^{3+} and shaken for 24 h at 30°C. The supernatant was decanted and the resin spheres were rinsed using ultrapure water. Then, resin spheres were reduced by freshly prepared 100 mL of 1% $NaBH_4$ solution with constant stirring under the N_2 atmosphere for 2 h at 25°C. The products were washed with deoxygenated ethanol and vacuum dried at 40°C. The obtained NZVI-resin composites were called NZVI-R1, NZVI-R2 and NZVI-R3, corresponding to 0:100, 30:70 and 70:30 (v/v) ethanol-water mixed solvent used to prepare the Fe^{3+} solution, respectively.

2.3 Characterization of NZVI-R

High-resolution transmission electron microscope (HR-TEM) images were taken on a JEM-2100 electron microscope at 200 kV. The particle size distribution and mean diameter of zero valent iron particles were analyzed using image analysis software Image J 2x (http://rsb.info.nih.gov/ij/index.html). X-ray photoelectron spectroscopy was obtained using a PHI5000 VersaProbe to characterize the surface chemistry of the material.

2.4 Batch experiments for bromate reduction

All the batch experiments were carried out in three-neck flasks at 25°C within a water bath incubator. A certain amount of NZVI-resin composites were added into 2000 mL bromate solution (1 $mg \cdot L^{-1}$) with the rotation speed of 200 $r \cdot min^{-1}$. To keep an identical amount of NZVI in the bromate solution (29.15 $mg \cdot L^{-1}$), different doses of the NZVI-resin composites were added (0.8917 g, 0.5589 g and 0.4546 g for NZVI-R1, NZVI-R2 and NZVI-R3, respectively). At specific time interval, aliquots of supernatant were sampled with a syringe, and filtered through a 0.22 μm membrane filter before analysis. Bromate and bromide were measured to get a time-dependent profile. All samples were prepared in duplicate, and mean values were reported.

To quantitatively evaluate the reduction reactivity, the pseudo-first-order kinetic model was used to describe the kinetics of bromate reduction by three NZVI-resin composites.

$$\frac{d[BrO_3^-]}{dt} = K_{obs}[BrO_3^-], \quad (1)$$

$$\ln\left(\frac{[BrO_3^-]_0}{[BrO_3^-]_t}\right) = K_{obs}t, \quad (2)$$

where $[BrO_3^-]_t$ is the concentration of bromate ($mg \cdot L^{-1}$) at time t, $[BrO_3^-]_0$ is the initial concentration of bromate ($mg \cdot L^{-1}$), K_{obs} is the observed pseudo-first-order rate constant (min^{-1}) and can be calculated from liner regression of $\ln([BrO_3^-]_0/[BrO_3^-]_t)$ versus time.

2.5 Chemical analysis

The concentration of bromate and bromide was measured using an ion chromatograph (Dionex ICS 1000, California, USA) with an IonPacAS11-HC (4 mm × 250 mm) analytical column and an AG11-HC guard column, respectively. The mobile phase is 15 $mmol \cdot L^{-1}$ KOH solution at a flow rate of 1.0 $mL \cdot min^{-1}$. The Fe loaded onto the resin was eluted by H_2SO_4 (10 wt.%) first and then analyzed by atomic absorption spectrophotometer (SHIMADZU AA-6300C, Japan) to determine the loading quantity of Fe on the resin.

3 Results and discussion

3.1 Characterization of the NZVI-resin composites

3.1.1 Fe loading quantity

The Fe content of three NZVI-resin composites is 69.9 mg $\cdot g^{-1}$, 116.5 $mg \cdot g^{-1}$ and 147.1 $mg \cdot g^{-1}$, respectively, which increased with increasing the proportion of ethanol in the ethanol-water mixed solvent for preparing the Fe^{3+}

solution. It is well known that DOW 3N retains Fe^{3+} ions mainly by formation of nitrogen atoms-Fe^{3+} complexes [29,30]. However, water molecular can also be adsorbed strongly onto pyridinic nitrogen by hydrogen bond, and has a negative competitive effect on adsorption of iron ion. Consequently, the amount of iron ion chelated on resin would increase when water was replaced by ethanol-water co-solvent for dissolving the ferric sulfate (Table S2 of Supplementary material). Therefore, much higher Fe loading was obtained when ethanol-water mixture replaced water as solvent for preparing the ferric sulfate solution.

3.1.2 TEM morphology and NZVI particles size distribution

TEM images were used to illustrate the morphology and particle size of NZVI particles loaded on the DOW 3N resin. It was shown clearly in Fig. 1 that the NZVI was spherical shaped (but not regular) particles, and the size of NZVI particles was closely related to the Fe loading quantity on DOW 3N resin. When the Fe content in composite was 69.9 $mg \cdot g^{-1}$, the NZVI particles ranged mainly from 5 to 10 nm in diameter were well dispersed with mean particle size of 11.30 nm. When the Fe content was increased from 69.9 $mg \cdot g^{-1}$ to 116.5 $mg \cdot g^{-1}$, the mean diameter of NZVI particles was increased to 12.96 nm, moreover, the whisker structure was found, which was also reported by Wang et al. [31]. Compared with NZVI-R1, the NZVI particles ranged from 5 to 10 nm in the NZVI-R2 was decreased; however, these in the range of 10 to 20 nm were increased obviously, moreover, the NZVI particles in the range of 40 to 50 nm can be observed. When the Fe content was increased further to 147.1 $mg \cdot g^{-1}$, the NZVI particles less than 5–10 nm disappeared, and the mean particle diameter was increased to 34.39 nm. This is because more Fe^0 crystal nucleuses would be formed during $NaBH_4$ reduction process when the amount of the precursor Fe^{3+} on the DOW 3N was increased, leading to higher probability of nucleus particle aggregation and thus formation of larger size particles. The result was in good agreement with results of some other researches [20,32], that the particle size of NZVIs was in direct proportion to the population of precursor Fe^{3+}.

3.1.3 XPS analysis

Figure 2 showed XPS Fe 2p spectra of NZVI-R composites. The photoelectron peaks at 705.96 eV and 718.92 eV were assigned to the binding energies of $Fe(2p_{3/2})$ and $Fe(2p_{1/2})$ of Fe^0, respectively, confirming that NZVI particles were successfully attached on the resin by the liquid phase reduction method. The presence of peaks at binding energies of $Fe(2p_{3/2})$ and $Fe(2p_{1/2})$ corresponded to 709.84 eV and 723.42 eV were attributed to the oxidized iron species [33], which may be formed on the surface of NZVI during the vacuum freeze drying process.

3.2 Bromate reduction using NZVI-R

The removal efficiency of bromate by three NZVI-R composites was investigated in Fig. 3. The removal efficiency declined progressively with the increase of Fe loading on resin. NZVI-R1 showed the highest removal efficiency of about 100% toward bromate after 180 min, while the removal efficiency was 93.9% and 74.9% by NZVI-R2 and NZVI-R3, respectively. The bromate removal by supporter DOW 3N resin at the same amount as that used in preparing NZVI-R2 was tested (not shown). Only 46.1% of bromate was removed by DOW 3N and lower than 93.9% by NZVI-R2. Moreover, bromide was not detected, which was considered to be only reduction product during the reduction of bromate using zero-valent iron [15,17]. The reduction reaction of bromate by zero-valent iron may be expressed by Eq. (1) and (2). Based on the results, it can be concluded that DOW 3N resin did not have a direct contribution to bromate reduction.

$$BrO_3^- + 3Fe^0 + 3H_2O \rightarrow Br^- + 3Fe^{2+} + 6OH^- \quad (3)$$

$$BrO_3^- + 2Fe^0 + 3H_2O \rightarrow Br^- + 2Fe^{3+} + 6OH^- \quad (4)$$

The bromide produced during the removal of bromate by three NZVI-R composites was also shown in Fig. 3. The concentration of bromide was decreased with the increase of Fe loading on resin. The mass balance of total bromine was calculated and shown in Fig. S1 (Supplementary Material). About 80% bromine recovery was obtained for all the three samples. The bromine recovery rate of less than 100% was mainly attributable to bromide adsorption onto the pyridine groups and iron oxides of NZVI-resin composites [17]. In sum, the removal of bromate was dominantly due to the reduction by NZVI instead of adsorption by DOW 3N.

It can be learned from Fig. 3 that three NZVI-resin composites had the different reduction reactivity for bromate. The most likely reason was that the nano iron particles loaded in resin had different size. The reduction of contaminants by ZVI is a surface reaction [15], therefore, the smaller nano iron particles has higher surface reactivity due to larger specific surface area [34]. As discussed above, the order of the mean NZVI particles size of three samples was NZVI-R1 < NZVI-R2 < NZVI-R3. Therefore, the removal efficiency followed the order: NZVI-R1 > NZVI-R2 > NZVI-R3.

As shown in Fig. S2, the kinetics of bromate removal by NZVI-resin composites can be described by pseudo-first-order model very well with a correlation coefficient (R^2) higher than 0.985. Value of K_{obs} was an indicator to compare the reactivity. The calculated K_{obs} followed the sequence of NZVI-R1 > NZVI-R2 > NZVI-R3, confirm-

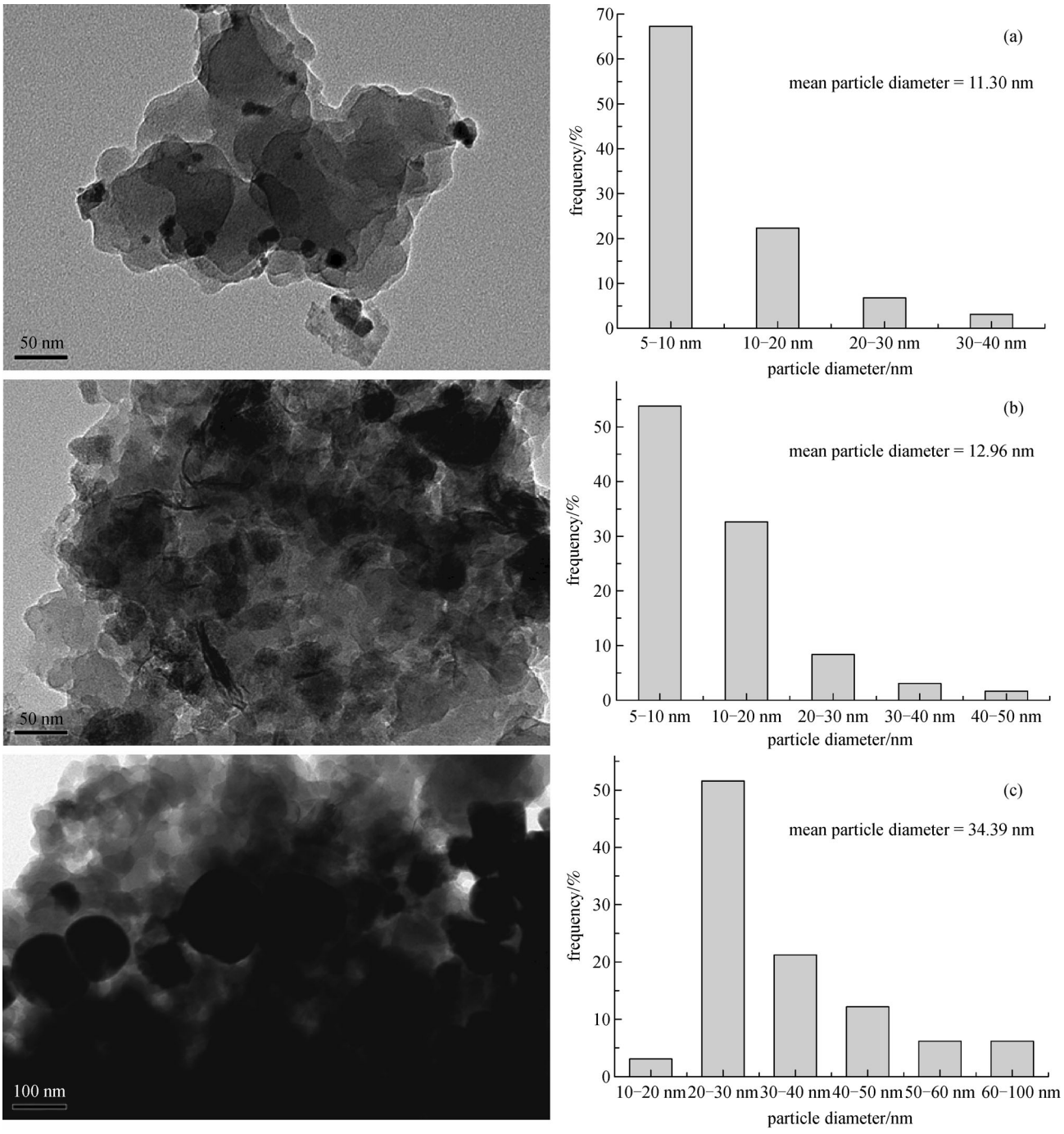

Fig. 1 TEM images and size distribution of NZVI nanoparticles: (a) NZVI-R1, (b) NZVI-R2 and (c) NZVI-R3

ing that the smaller nano iron particles has higher reduction reactivity for bromate.

3.3 Effect of DO on NZVI-R reactivity

The effect of dissolved oxygen (DO) concentrations on the removal of bromate by three NZVI-resin composites was investigated and shown in Fig. 4. The pseudo-first-order reaction constants (K_{obs}) and R^2 for bromate removal by three NZVI-resin composites were summarized in Table S3 (Supplementary Material). The K_{obs} kept the same sequence: NZVI-R1 > NZVI-R2 > NZVI-R3 at the DO concentrations of 0–0.1 mg·L^{-1}, 5±0.1 mg·L^{-1} and 9.0±0.1 mg·L^{-1}. That is to say, the increase of DO concentration would decrease the bromate removal efficiency for three NZVI-resin composites, which was consistent with other reports [35]. The decline in removal efficiency was likely due to the competition between

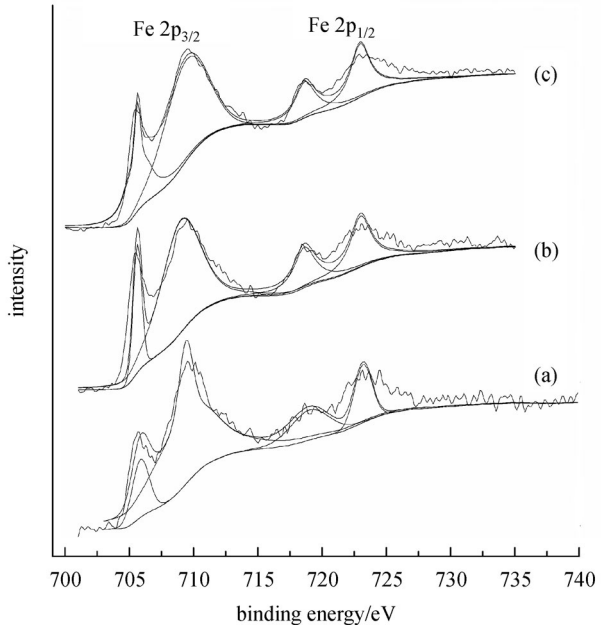

Fig. 2 XPS Fe 2p spectra of (a) NZVI-R1, (b) NZVI-R2 and (c) NZVI-R3

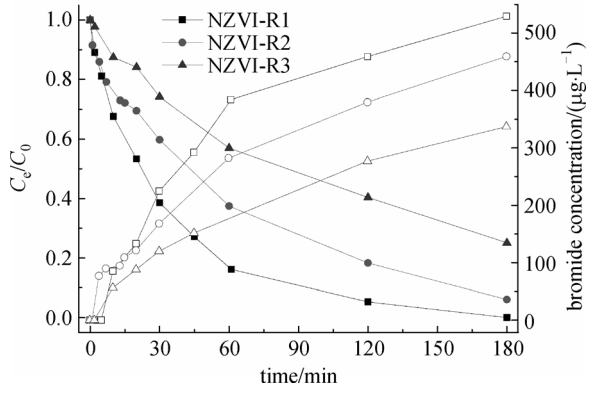

Fig. 3 Bromate removal by NZVI-R1 (■□), NZVI-R2 (● ○), NZVI-R3 (▲△). Filled symbols denote bromate, and open symbols denote bromide. (Iron dosage = 29.15 mg·L^{-1}, BrO_3^- = 1 mg·L^{-1}, pH = 6.1, DO = 9.0±0.1 mg·L^{-1} and rotation speed = 200 r·min^{-1})

oxygen and bromate for effective reactive sites and deactivation of the NZVI particles surface by forming a passive iron oxide layer [36].

Figure 5 showed the effect of the DO concentration on K_{obs} for each NZVI-resin composite. It can be found there was a good linear relationship between the DO and K_{obs}, however, the slope values for three composites were different; namely, the effect of the DO on the reactivity of NZVI-resin composites with different Fe loading was different. The slope value for NZVI-R1 and NZVI-R2 (0.0049 and 0.0051, respectively) was larger than that for NZVI-R3 (0.0025), indicating that DO had the minimal impact on bromate removal by NZVI-R3 with the largest Fe loading. It was possibly because that NZVI-R3 had the biggest mean particle size of NZVIs (34.39 nm) and thus the weakest reduction activity. The NZVI particles size within NZVI-R1 and NZVI-R2 (11.30 nm and 12.96 nm, respectively) was much smaller than that within NZVI-R3, resulting in lower reduction activity for bromate. Therefore, an obvious effect of DO on bromated removal by NZVI-R1 and NZVI-R2 can be observed.

3.4 Effect of pH on NZVI-R reactivity

The effect of initial pH on bromate removal was studied by changing the initial solution pH between 4.5 and 9.5 in Fig. 6, the removal efficiency of bromate was 100.0% after 180 min by the three NZVI-resin composites when the initial pH was 4.5. Also, it can be learned that the removal efficiency decreased with the increase of the initial solution pH, and the reduction of bromated by the NZVI-resin composites was highly pH-dependent. When the initial pH value was increased to 9.5, the removal of bromate dropped to 91.4%, 71.9% and 52.5% for NZVI-R1, NZVI-R2 and NZVI-R3, respectively. The possible reason is that high pH can promote the formation of ferrous hydroxide and other protective layers on the surface of NZVI, and thus reduces fresh active sites. So the removal efficiency decreased dramatically when the solution pH varied from 4.5 to 9.5.

The reaction kinetics at different initial pH values obeyed the pseudo-first-order model. Table S4 (Supplementary Material) showed the pseudo-first-order reaction constants (K_{obs}) and R^2 for bromate removal by the three NZVI-resin composites under various initial pH values. To learn the effect of the initial pH on bromate removal by different NZVI-resin composites, the plots of reaction constants (K_{obs}) *vs.* pH were shown in Fig. 7. It can be seen from Fig. 7 that the K_{obs} was almost unchanged for three NZVI-resin composites between the pH of 6.1 and 8.0. When the initial pH decreased from 6.1 to 4.5, the value of K_{obs} increased for all the NZVI-R composites, but the degrees were different. It is very interesting to found that the increase in K_{obs} was positively correlated with the Fe loading quantity and mean NVZI particle size. When the initial pH decreased from 6.1 to 4.5, the K_{obs} increase by 1.58, 2.56 and 3.18 times for NZVI-R1, NZVI-R2 and NZVI-R3 respectively. This result may be explained as follows: when the initial pH decreased from 6.1 to 4.5, due to the largest particle size and the weakest reaction activity, it is reasonable that the value of K_{obs} increased the most significantly for NZVI-R3. In addition, when the initial pH increased from 8.0 to 9.5,the value of K_{obs} decreased by 42.17%, 39.40%, and 34.67% for NZVI-R1, NZVI-R2, NZVI-R3, respectively, which was negatively correlated to the Fe loading quantity and mean NVZI particle size. In the alkaline solution, Fe^{2+} ions from the iron surface and hydroxyl ions reacted to precipitate ferrous hydroxide on

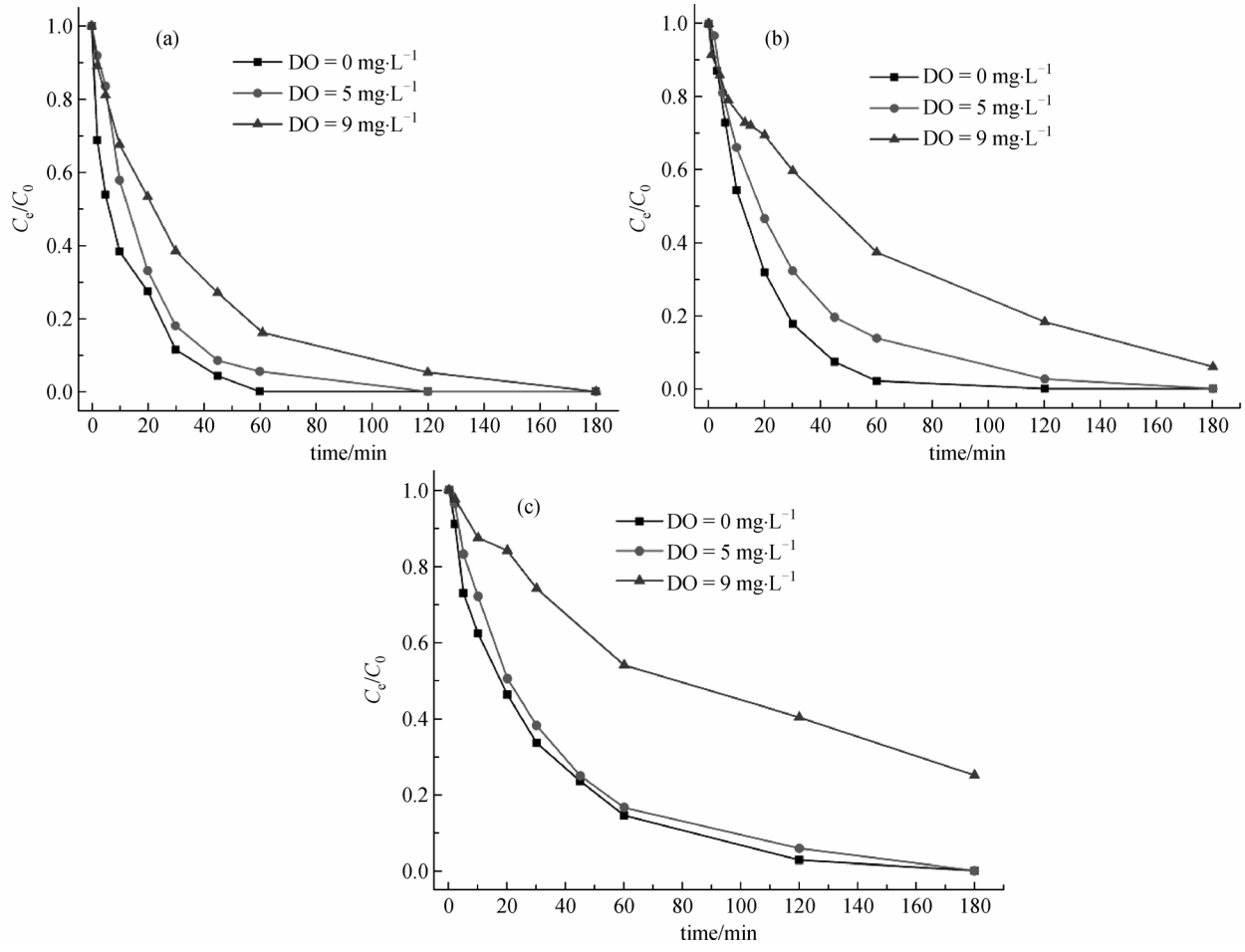

Fig. 4 Effect of dissolved oxygen on bromate removal by NZVI-resin composites under various DO concentrations: (a) NZVI-R1, (b) NZVI-R2 and (c) NZVI-R3 (iron dosage = 29.15 mg·L^{-1}, BrO_3^- = 1 mg·L^{-1}, pH = 6.1 and rotation speed = 200 r·min^{-1})

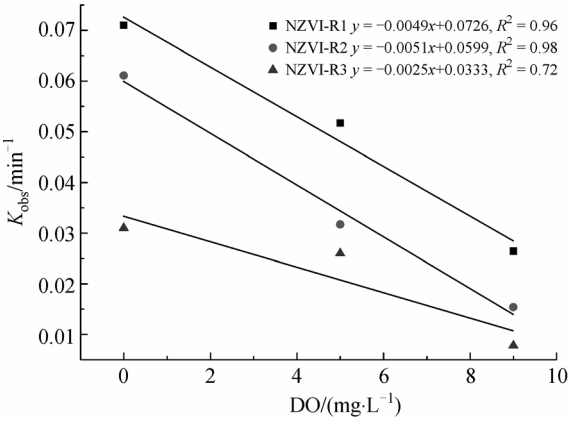

Fig. 5 The linear fitting results of K_{obs} under different DO concentration

the surface of the iron occupying the reactive sites, thus hindering the reaction. Due to the smallest particle size and the strongest reaction activity for NZVI-R1, therefore, there was the largest decrease in K_{obs} value when the initial pH increased from 8.0 to 9.5.

3.5 Effect of co-existing anions on NZVI-R reactivity

The effects of co-existing anions NO_3^-, PO_4^{3-} and HCO_3^- on bromate removal by three NZVI-R composites were investigated and showed in Fig. 8. The concentrations of NO_3^-, PO_4^{3-} and HCO_3^- were 10 mg N·L^{-1}, 0.5 mg P·L^{-1} and 60 mg·L^{-1}, respectively. The reaction rate constants of bromate reduction by NZVI-R composites with different co-existing anions were shown in Table S5. We can conclude from Fig. 8 that NO_3^- and PO_4^{3-} exhibited dramatically adverse effects on bromate reduction by NZVI-R, while HCO_3^- only showed slightly adverse effect on bromate reduction. In the presence of nitrate, both of the reaction rates and the removal efficiency of bromate were declined. As a reactant, nitrate not only slowed the reduction of bromate by competing for reactive sites on the iron but also reduced reactivity by serving as a passivating agent [37]. The inhibition of phosphate to the

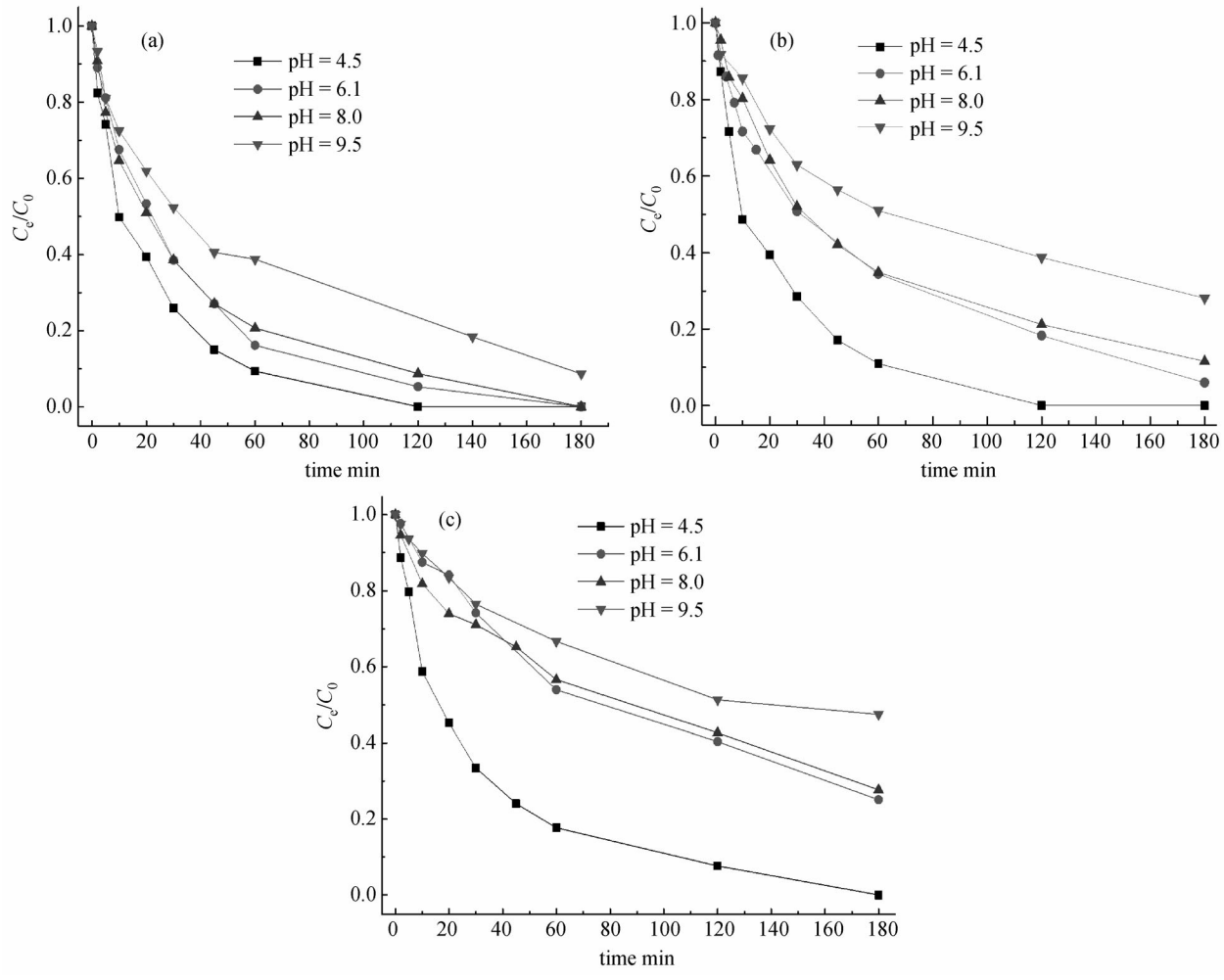

Fig. 6 Effect of pH on bromate removal by NZVI-resin composites under various initial pH: (a) NZVI-R1, (b) NZVI-R2 and (c) NZVI-R3 (iron dosage = 29.15 mg·L^{-1}, BrO_3^- = 1 mg·L^{-1}, DO = 9.0±0.1 mg·L^{-1} and rotation speed = 200 r·min^{-1})

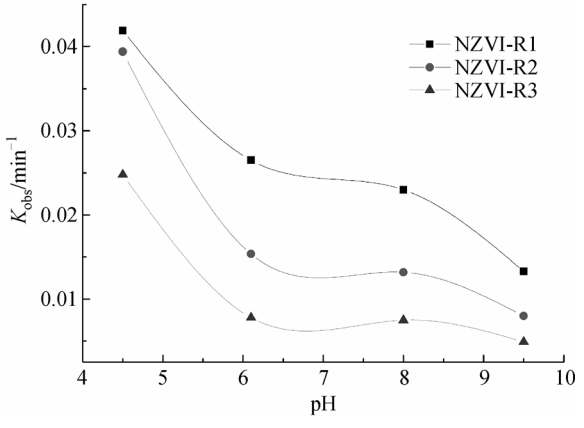

Fig. 7 Reaction rate constants of bromate removal by NZVI-resin composites under various initial pH values

bromate reduction was mainly due to the adsorption or co-precipitation of phosphate on the iron surface through the formation of complexes with iron and iron oxides. The adsorption of phosphate could occupy the available active sites and thus lower the bromate removal efficiency [15]. Bicarbonate had slightly inhibitory effect on the bromate reduction as shown in Fig. 8 and Table S5. However, some reports reviewed the presence of carbonate could enhance the reactivity of Fe^0 [38,39]. The inhibition of bicarbonate to the bromate reduction in our study was possibly due to the precipitation as siderite, iron carbonate hydroxides, aragonite, or calcite and the formation of an insulating film on the iron surface [40,41].

4 Conclusions

In this study, the NZVI supported on DOW 3N with three different Fe loading was prepared. The mean diameter of the NZVI particles increased with increasing the Fe loading on DOW 3N. The NZVI-resin composites with lower Fe loading quantity showed higher reduction

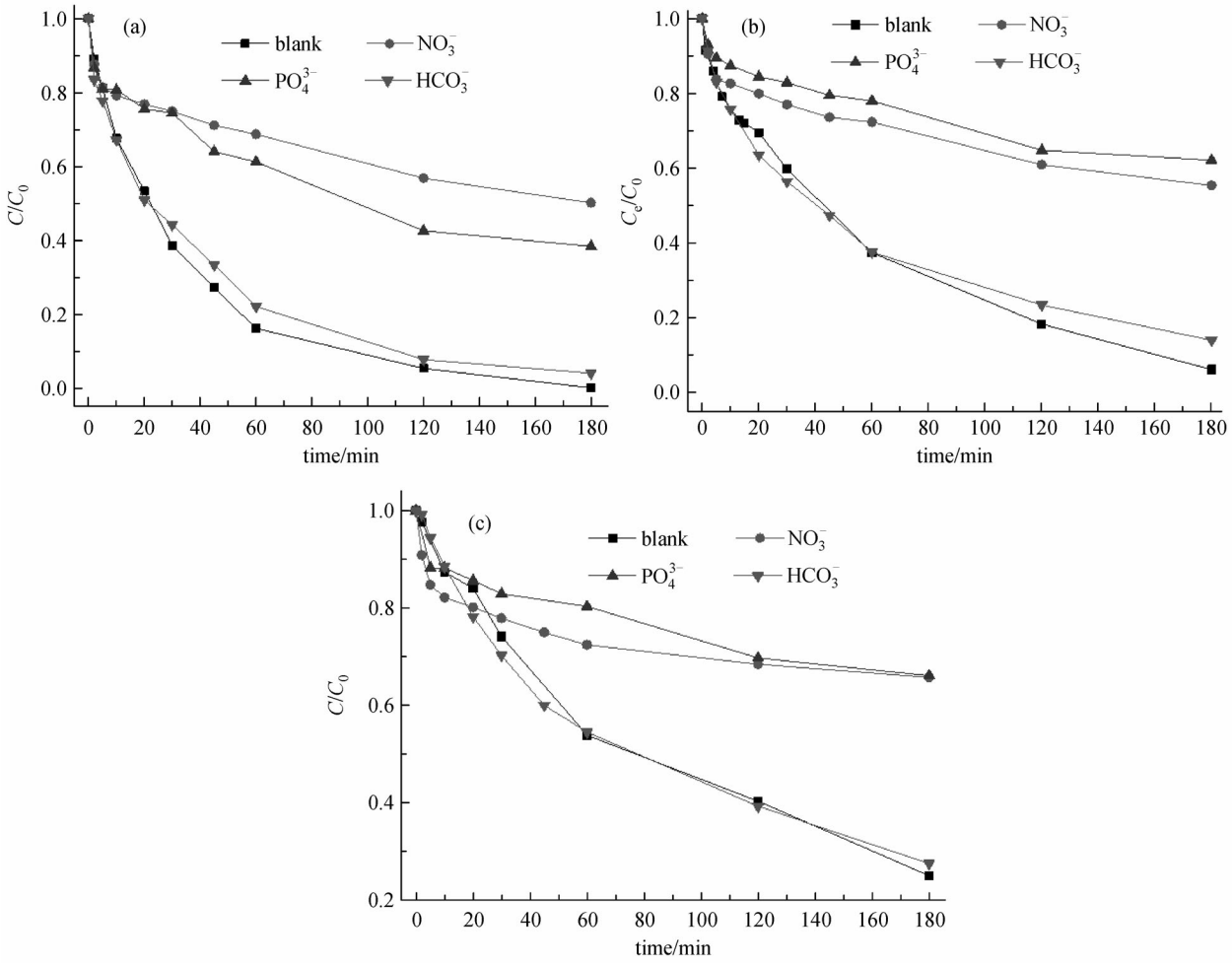

Fig. 8 Effect of co-existing anions on bromate removal by NZVI-resin composites: (a) NZVI-R1, (b) NZVI-R2 and (c) NZVI-R3 (iron dosage = 29.15 mg·L^{-1}, BrO_3^- = 1 mg·L^{-1}, pH = 6.1, DO = 9.0±0.1 mg·L^{-1} and rotation speed = 200 r·min^{-1})

reactivity for bromated due to smaller particles size of NZVI. Under the same operational conditions, the results of batch experiments indicated that almost 100.0% of bromate removal was reached by NZVI-resin composite loaded with 69.9 mg·g^{-1} Fe, while 93.9% and 74.9% by NZVI-resin composites loaded with 116.5 and 147.1 mg·g^{-1} Fe, respectively. The effect of DO concentration on bromate removal was negatively correlated to Fe loading quantity. Decreasing the pH value could enhance the removal efficiency. Under acidic conditions, decreasing the pH value had the most significant influence on NZVI-R3 with highest Fe loading (147.1 mg·g^{-1}) for bromate removal; however, under alkaline conditions, the most significant influence of pH was on NZVI-R1 with lowest Fe loading (69.9 mg·g^{-1}). The co-existing anions NO_3^-, PO_4^{3-} and HCO_3^- showed adverse effects on bromate reduction by NZVI-R. The possible reason was due to the reduction of NO_3^- and the adsorption or co-precipitation of phosphate and bicarbonate on the surface of Fe^0.Taken together, it is important to optimize the Fe loading quantity on NZVI-resin composites for the bromate removal.

Acknowledgements This research was financially funded by Program for New Century Excellent Talents in University (Grant No. NCET-11-0230), Major Special Project of Water Pollution Control and Management Technology of China (Grant No. 2012ZX07101-003) and Program for Changjiang Scholars Innovative Research Team in University.

Supplementary material is available in the online version of this article at http://dx.doi.org/10.1007/s11783-015-0781-2 and is accessible for authorized users.

Reference

1. Liu Y, Lowry G V. Effect of particle age (Fe^0 content) and solution pH on NZVI reactivity: H_2 evolution and TCE dechlorination. Environmental Science & Technology, 2006, 40(19): 6085–6090
2. Liu Y, Majetich S A, Tilton R D, Sholl D S, Lowry G V. TCE dechlorination rates, pathways, and efficiency of nanoscale iron particles with different properties. Environmental Science & Technology, 2005, 39(5): 1338–1345
3. Shu H Y, Chang M C, Chen C C, Chen P E. Using resin supported nano zero-valent iron particles for decoloration of Acid Blue 113 azo

dye solution. Journal of Hazardous Materials, 2010, 184(1–3): 499–505

4. Lowry G V, Johnson K M. Congener-specific dechlorination of dissolved PCBs by microscale and nanoscale zerovalent iron in a water/methanol solution. Environmental Science & Technology, 2004, 38(19): 5208–5216
5. Zhu S N, Liu G H, Ye Z, Zhao Q, Xu Y. Reduction of dinitrotoluene sulfonates in TNT red water using nanoscale zerovalent iron particles. Environmental Science and Pollution Research International, 2012, 19(6): 2372–2380
6. Zhang X, Lin S, Lu X Q, Chen Z L. Removal of Pb(II) from water using synthesized kaolin supported nanoscale zero-valent iron. Chemical Engineering Journal, 2010, 163(3): 243–248
7. Li X Q, Zhang W X. Iron nanoparticles: the core-shell structure and unique properties for Ni(II) sequestration. Langmuir, 2006, 22(10): 4638–4642
8. Uezuem C, Shahwan T, Eroglu A E, Hallam K R, Scott T B, Lieberwirth I. Synthesis and characterization of kaolinite-supported zero-valent iron nanoparticles and their application for the removal of aqueous Cu^{2+} and Co^{2+} ions. Applied Clay Science, 2009, 43(2): 172–181
9. Shi L N, Zhou Y, Chen Z, Megharaj M, Naidu R. Simultaneous adsorption and degradation of Zn^{2+} and Cu^{2+} from wastewaters using nanoscale zero-valent iron impregnated with clays. Environmental Science and Pollution Research International, 2013, 20(6): 3639–3648
10. Cao J S, Elliott D, Zhang W X. Perchlorate reduction by nanoscale iron particles. Journal of Nanoparticle Research, 2005, 7(4–5): 499–506
11. Xiong Z, Zhao D, Pan G. Rapid and complete destruction of perchlorate in water and ion-exchange brine using stabilized zero-valent iron nanoparticles. Water Research, 2007, 41(15): 3497–3505
12. Hwang Y H, Kim D G, Shin H S. Mechanism study of nitrate reduction by nano zero-valent iron. Journal of Hazardous Materials, 2011, 185(2–3): 1513–1521
13. Sohn K, Kang S W, Ahn S, Woo M, Yang S K. Fe^0 nanoparticles for nitrate reduction: stability, reactivity, and transformation. Environmental Science & Technology, 2006, 40(17): 5514–5519
14. Westerhoff P. Reduction of nitrate, bromate, and chlorate by zero valent iron (Fe^0). Journal of Environmental Engineering, 2003, 129 (1): 10–16
15. Xie L, Shang C. The effects of operational parameters and common anions on the reactivity of zero-valent iron in bromate reduction. Chemosphere, 2007, 66(9): 1652–1659
16. Wu X, Yang Q, Xu D, Zhong Y, Luo K, Li X, Chen H, Zeng G. Simultaneous adsorption/reduction of bromate by nanoscale zero-valent iron supported on modified activated carbon. Industrial & Engineering Chemistry Research, 2013, 52(35): 12574–12581
17. Wang Q, Snyder S, Kim J, Choi H. Aqueous ethanol modified nanoscale zero-valent iron in bromate reduction: synthesis, characterization, and reactivity. Environmental Science & Technology, 2009, 43(9): 3292–3299
18. Alowitz M J, Scherer M M. Kinetics of nitrate, nitrite, and Cr(VI) reduction by iron metal. Environmental Science & Technology, 2002, 36(3): 299–306
19. Hwang Y H, Kim D G, Shin H S. Effects of synthesis conditions on the characteristics and reactivity of nano scale zero-valent iron. Applied Catalysis B: Environmental, 2011, 105(1–2): 144–150
20. He F, Zhao D. Manipulating the size and dispersibility of zero-valent iron nanoparticles by use of carboxymethyl cellulose stabilizers. Environmental Science & Technology, 2007, 41(17): 6216–6221
21. Zhu H, Jia Y, Wu X, Wang H. Removal of arsenic from water by supported nano zero-valent iron on activated carbon. Journal of Hazardous Materials, 2009, 172(2–3): 1591–1596
22. Choi H, Al-Abed S R. Effect of reaction environments on the reactivity of PCB (2-chlorobiphenyl) over activated carbon impregnated with palladized iron. Journal of Hazardous Materials, 2010, 179(1–3): 869–874
23. Zhang Y, Li Y, Li J, Hu L, Zheng X. Enhanced removal of nitrate by a novel composite: nanoscale zero-valent iron supported on pillared clay. Chemical Engineering Journal, 2011, 171(2): 526–531
24. Wang W, Zhou M H, Mao Q O, Yue J J, Wang X. Novel NaY zeolite-supported nanoscale zero-valent iron as an efficient heterogeneous Fenton catalyst. Catalysis Communications, 2010, 11(11): 937–941
25. Ponder S M, Darab J G, Bucher J, Caulder D, Craig I, Davis L, Edelstein N, Lukens W, Nitsche H, Rao L F, Shuh D K, Mallouk T E. Surface chemistry and electrochemistry of supported zerovalent iron nanoparticles in the remediation of aqueous metal contaminants. Chemistry of Materials, 2001, 13(2): 479–486
26. Jiang Z, Lv L, Zhang W, Du Q, Pan B, Yang L, Zhang Q. Nitrate reduction using nanosized zero-valent iron supported by polystyrene resins: role of surface functional groups. Water Research, 2011, 45 (6): 2191–2198
27. Shi J, Yi S, He H, Long C, Li A. Preparation of nanoscale zero-valent iron supported on chelating resin with nitrogen donor atoms for simultaneous reduction of Pb^{2+} and NO_3^-. Chemical Engineering Journal, 2013, 230: 166–171
28. Moore M M, Chen T. Mutagenicity of bromate: implications for cancer risk assessment. Toxicology, 2006, 221(2–3): 190–196
29. Diniz C V, Ciminelli V S T, Doyle F M. The use of the chelating resin Dowex M-4195 in the adsorption of selected heavy metal ions from manganese solutions. Hydrometallurgy, 2005, 78(3–4): 147–155
30. Diniz C V, Doyle F M, Ciminelli V S T. Effect of pH on the adsorption of selected heavy metal ions from concentrated chloride solutions by the chelating resin Dowex M-4195. Separation Science and Technology, 2002, 37: 3169–3185
31. Wang W, Jin Z H, Li T L, Zhang H, Gao S. Preparation of spherical iron nanoclusters in ethanol-water solution for nitrate removal. Chemosphere, 2006, 65(8): 1396–1404
32. Jia H, Gu C, Boyd S A, Teppen B J, Johnston C T, Song C, Li H. Comparison of reactivity of nanoscaled zero-valent iron formed on clay surfaces. Soil Science Society of America Journal, 2011, 75(2): 357–364
33. Tan B J, Klabunde K J, Sherwood P M A. X-ray photoelectron-spectroscopy studies of solvated metal atom dispersed catalysts. Monometallic iron and bimetallic iron cobal particles on alumina. Chemistry of Materials, 1990, 2(2): 186–191
34. Liou Y H, Lo S L, Kuan W H, Lin C J, Weng S C. Effect of

precursor concentration on the characteristics of nanoscale zero-valent iron and its reactivity of nitrate. Water Research, 2006, 40 (13): 2485–2492

35. Yin W, Wu J, Li P, Wang X, Zhu N, Wu P, Yang B. Experimental study of zero-valent iron induced nitrobenzene reduction in groundwater: the effects of pH, iron dosage, oxygen and common dissolved anions. Chemical Engineering Journal, 2012, 184: 198–204
36. Huang Y H, Zhang T C. Effects of dissolved oxygen on formation of corrosion products and concomitant oxygen and nitrate reduction in zero-valent iron systems with or without aqueous Fe^{2+}. Water Research, 2005, 39(9): 1751–1760
37. Devlin J F, Allin K O. Major anion effects on the kinetics and reactivity of granular iron in glass-encased magnet batch reactor experiments. Environmental Science & Technology, 2005, 39(6): 1868–1874
38. Agrawal A, Ferguson W J, Gardner B O, Christ J A, Bandstra J Z, Tratnyek P G. Effects of carbonate species on the kinetics of dechlorination of 1,1,1-trichloroethane by zero-valent iron. Environmental Science & Technology, 2002, 36(20): 4326–4333
39. Reardon E J. Anaerobic corrosion of granular iron: measurement and interpretation of hydrogen evolution rates. Environmental Science & Technology, 1995, 29(12): 2936–2945
40. Kober R, Schlicker O, Ebert M, Dahmke A. Degradation of chlorinated ethylenes by Fe^0: inhibition processes and mineral precipitation. Environmental Geology, 2002, 41: 644–652
41. Phillips D H, Gu B, Watson D B, Roh Y, Liang L, Lee S Y. Performance evaluation of a zero-valent iron reactive barrier: mineralogical characteristics. Environmental Science & Technology, 2000, 34(19): 4169–4176